Hot Corrosion Behaviour of NiCrFeNbMoTiAl Coating in Molten Salts at 700°c by Electrochemical Techniques

J.L.Tristancho-Reyes[1,2], J.G. Chacón-Nava[1], D.Y. Peña-Ballesteros[3], C. Gaona-Tiburcio[1],
J.G. Gonzalez-Rodriguez[4], A. Martínez-Villafañe[1], F. Almeraya-Calderón[1,]*

[1] Centro de Investigación en Materiales Avanzados, S.C. Grupo corrosión.
Miguel de Cervantes 120, Complejo Industrial Chihuahua, 31109, Chihuahua, Chih., México.
[2] Universidad Tecnológica de Pereira. Facultad de Ingeniería Mecánica. Grupo de Investigación en Materiales Avanzados. Vereda la Julita-Pereira-Risaralda- Colombia.
[3] Universidad Industrial de Santander. Escuela de Ingeniería Metalúrgica y Ciencia de Materiales. Grupo de Investigación en Corrosión. Bucaramanga-Santander-Colombia.
[4] Universidad Autónoma del Estado de Morelos, FCQI-CIICAP. Cuernavaca-Morelos. México.
[*] E-mail: facundo.almeraya@cimav.edu.mx

This research studied the behavior of NiCrFeNbMoTiAl metallic coating under corrosive attack by molten salts 80% $Na_2SO_4 - 20\% V_2O_5$ and $80\% K_2SO_4 - 20\% V_2O_5$ deposited by non-transfer arc plasma-assisted thermal spraying (APS) at a temperature of 700ºC. Corrosion rate were determined by means of linear polarization resistance (LPR), electrochemical techniques, and electrochemical impedance spectroscopy (EIS). The results obtained showed a high severity of attack from the $80\% Na_2SO_4 - 20\% V_2O_5$ mixture. Nyquist plots show a trend that the load transfer mechanism was the predominant factor in the process activation.

Keywords: Hot corrosion, Metallic Coatings, Plasma Thermal Spraying, Electrochemical Techniques.

1. INTRODUCTION

Hot corrosion is one of the greatest problems affecting the electric power generation industry, especially in steam generating equipment (boilers) operating at high temperatures (600 to 1100°C). Depending on the design of heat exchanging equipment (superheaters and reheaters), fine films of molten salts may form on the metallic surfaces on specific areas of these pieces of equipment causing a highly corrosive condition. [1–3]

During normal coal combustion - which has high contents of sodium (Na), potassium (K), sulphur (S), and vanadium (V) - vanadium vapors (V_2O_5) and sulphates from alkaline metals (Na_2SO_4 y K_2SO_4) are generated and react to form binary systems that suffer a eutectic reactions at a relatively low temperature (600°C) causing the fusion of the saline deposit and forming a stable electrolyte layer on the metallic surface. Vanadium compounds are very corrosive and stable under normal operating conditions of the boiler. [4–6]

Corrosion by molten salts is divided in two categories. [7–9]

Type I hot corrosion (HTHC): This mechanism was observed in a temperature interval ranging from 750ºC to 900º. When the saline deposit is completely liquid the maximum corrosion rate appears over 900°C.

Type II hot corrosion (LTHC): it ranges from 650ºC to 750ºC, where the liquid phase of salt is formed only by the dissolution of several corrosion products, below the fusion point of pure Na_2SO_4 and is characterized by a non-uniform attack (pitting). The nature of pitting is related to localized oxide failure and is a consequence of thermal cycle caused by the mixture of salts.

A common model for the occurrence of Type II hot corrosion was suggested by Luthra [10–12] who states that type II hot corrosion follows two stages: the first of them presents the formation of a sulphate – liquid vanadium sulphate on the metallic surface; and the second stage in which there is propagation of the attack by migration of SO_3 within the metallic surface and the metallic ion towards the exterior through the salt film.

Plasma-assisted thermal projection with non-transferred arc (APS) [13–14] is a technology that may help solve superficial problems caused by molten salts corrosion, by applying metallic, ceramic, or composite protective coatings that act as thermal barriers.

The aim of this study is to assess the NiCrFeNbMoTiAl coating by means of electrochemical techniques in the presence of the molten salts 80wt. %V_2O_5– 20wt. % Na_2SO_4 and 80wt.%V_2O_5 – 20wt.% K_2SO_4 at 700°C.

2. EXPERIMENTAL PROCEDURE

In order to determine the electrochemical behavior of corrosion by molten salts in protective metallic coatings, cylindrical test pieces of 5mm in diameter, 25mm height were made of SA213 – T22 (2 ¼ Cr -1Mo) steel. The composition obtained by atomic absorption spectroscopy, shown in Table 1. This type of steel is commonly used in thermal power generation plants.

Table 1. Chemical composition of the SA 213-T22 alloy

%Cr	%C	%Mn	%Mo	%P	%S	%Si	%Fe
2.18	0.09	0.48	0.93	0.016	0.01	0.30	Balance

The metallic coating NiCrFeNbMoTiAl was applied on the test pieces by thermal projection with non-transferred arc plasma (APS), having a density of 4.08 g/cm^3 and particle sizes of -90μm/+45μm. Table 2 shows its chemical composition. These coated test pieces were subject to corrosive attack in saline mixtures of 80wt. %V_2O_5– 20wt. % Na_2SO_4 and 80wt.%V_2O_5 – 20wt.% K_2SO_4 at a temperature of 700ºC.

Table 2. Chemical composition of the NiCrFeNbMoTiAl coating

%Ni	%Cr	%Fe	%Nb	%Mo	%Ti	%Al
Balance	19	18	5	3	1	0.5

The corrosion cell is made up of a three-electrode arrangement; the SA213-T22 steel work electrode coated with NiCrFeNbMoTiAl as a reference electrode and as counter electrode a high purity platinum wire, 1mm in diameter embedded in quartz tubes sealed with ceramic cement. The experimental device was introduced in a furnace for temperature corrosion tests.

The salts mixtures used were 80wt. %V_2O_5– 20wt. % Na_2SO_4 and 80wt.%V_2O_5 – 20wt.% K_2SO_4 analytic degree, thus guaranteeing their high purity. These two mixtures simulate the behaviour of ashes produced from the combustion in boilers of thermoelectric centrals. The amount of mixture used for each assay was 30 grams.

The electrochemical parameters were as follows: for linear polarization resistance technique, the $\pm$20 mV potential was polarized regarding the balance potential at a speed of 10mV/min., [15–16]; and for the electrochemical impedance spectroscopy (EIS) a frequency sweep from 0.01 to 10,000 Hz and amplitude of 10mV was made [17–19]. The coating was characterized by means of scanning electron microscopy (SEM) before and after undergoing the corrosive attack by molten salts.

3. RESULTS AND DISCUSSION

The morphology of the metallic coating NiCrFeNbMoTiAl layer, sprayed by means of APS on SA213-T22 steel (Figure 1) was obtained by scanning electron microscopy (SEM) before the corrosive attack tests by molten salts, observing a dense, slightly porous, homogenous layer with good adherence.

Table 3 groups the polarization resistance (Rp), corrosion current (I_{Corr}) and corrosion rate (CR) for each mixture of salt at the test temperature. Figures 2 and 3 shows the polarization resistance diagrams obtained from samples exposed to corrosive attack by molten salts the protective layers of metallic coating NiCrFeNbMoTiAl at 700°C.

From the results obtained from the linear polarization resistance technique (LPR), a lesser value of polarization resistance (Rp) was observed by the coating layer exposed to corrosive attack by molten salts in the 80%V_2O_5 – 20%Na_2SO_4 mixture as a consequence of the increase in the concentration of electro active species which are very aggressive and have a conductive nature. [4]
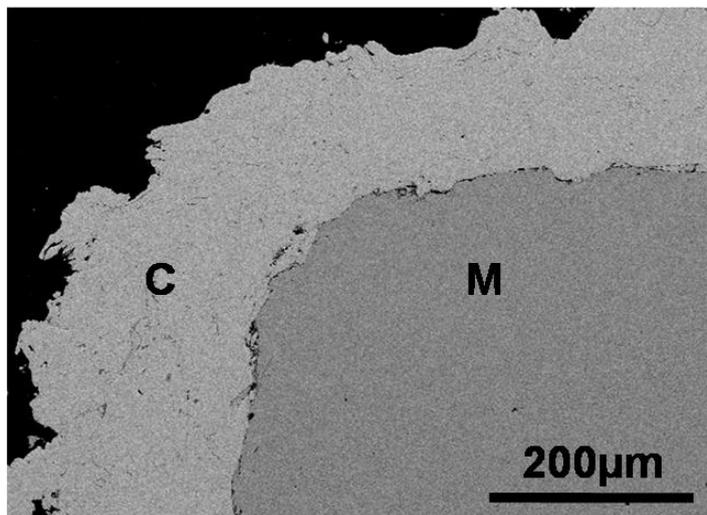
Figure 1. SEM micrograph of the coating before test. C=Coating, M=Matrix

Table 3. Polarization resistence (rp), corrosion current (i_{corr}) and corrosion rate (cr) values at 700°c

Mixture.	Rp ($\Omega.m^2$)	I_{CORR} (mA/cm^2)	CR (mm/y)
80% V_2O_5 − 20% Na_2SO_4	0.0000646	0.0244	0.494
80% V_2O_5 − 20% K_2SO_4	0.0001416	0.00576	0.117

The corrosion rate values were determined by using the Stern and Geary equation, Equation (1). [20]

$$Rp = \beta / I_{CORR}$$

Equation (1)

Were:

Rp = Polarization Resistance ($\Omega.cm^2$).

β = Tafel's constant (V).

I_{Corr} = corrosion current ($\mu A/cm^2$).

Therefore, the corrosion rate is given by, Equation (2):

$$CR = 3.27x10^{-3} \left(\frac{I_{CORR} \; x \; E.W}{\rho} \right)$$

Equation (2)

Where:

CR = Corrosion Rate (mm/year).

I_{Corr} = Corrosion current ($\mu A/cm^2$).
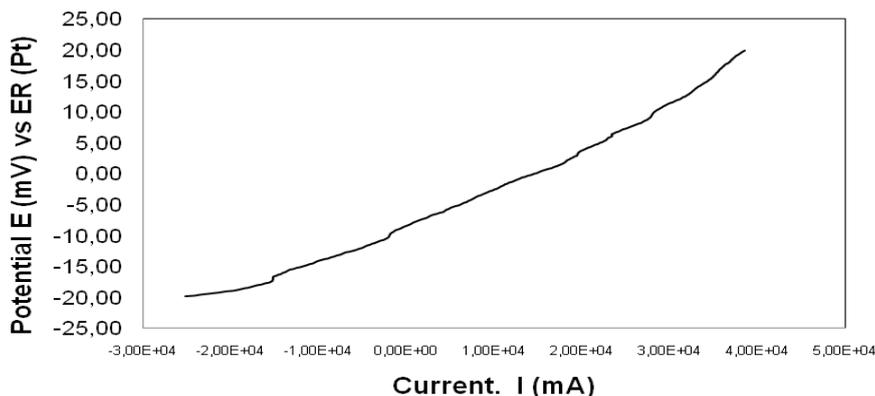
EW. = Equivalent weight (g).

ρ = Density (g/cm^3).

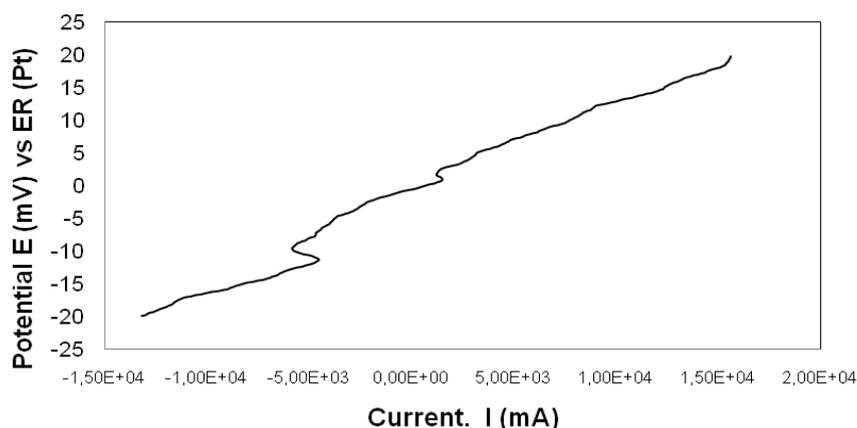**Figure 2.** Polarization resistance diagram at 700°C in $80\% \, V_2O_5 - 20\% \, Na_2SO_4$**.**

Figure 3. Polarization resistance diagram at 700°C in $80\% \, V_2O_5 - 20\% \, K_2SO_4$

Table 4. Charge transfer resistance (rct), corrosion current (i_{corr}) and corrosion rate (cr) values at 700°c

Mixture	Rp ($\Omega.m^2$)	I_{CORR} (mA/cm^2)	CR (mm/y)
$80\% \, V_2O_5 - 20\% \, Na_2SO_4$	0.0000378	0.0417	0.843
$80\% \, V_2O_5 - 20\% \, K_2SO_4$	0.000110	0.0074	0.150

Table 4 shows the results of Charge Transfer Resistance (Rct), corrosion current (I_{Corr}) and corrosion rate (CR) obtained from the electrochemical impedance spectroscopy (EIS) technique. Figure 3 shows the Nyquist plots obtained by exposing the NiCrFeNbMoTiAl coating layer to corrosive attack by molten salts at 700°C.

A lesser charge transfer resistance value was observed in the results obtained in the $80\% \, V_2O_5 - 20\% \, Na_2SO_4$ mixture, thus the corrosive attack becomes more sever on the coating layer. In the Nyquist plots in figures 4 and 5, there is the presence of two semi circles, one at low frequencies, reflecting the behaviour of the metallic coating layer from which the coating resistance value is

determined, and other at high frequencies indicating the behaviour of the double electrical layer, from which the solution resistance and load transfer resistance values are obtained. These values become important when it comes to determine the rate of corrosion and to predict in this manner the behaviour of the metallic coating after exposure to corrosion by molten salts.
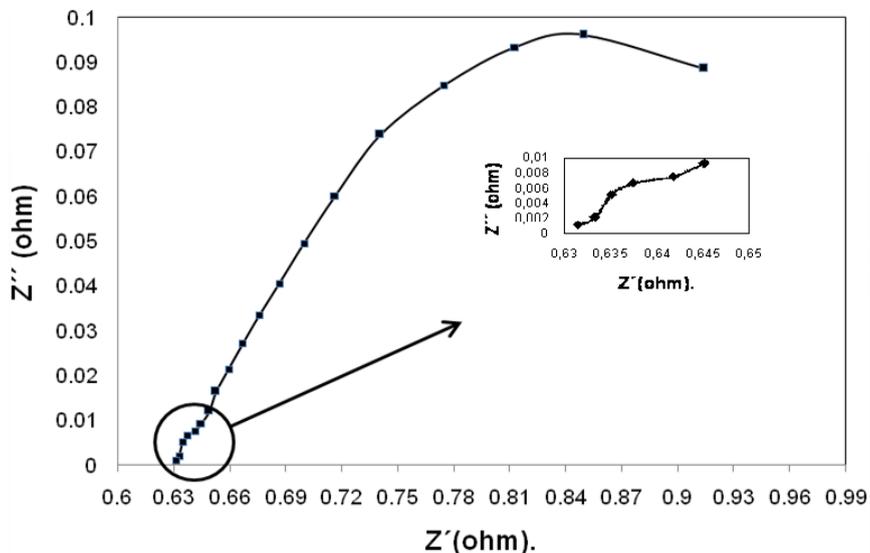

Figure 4. Nyquist Plots at 700°C, for the NiCrFeNbMoTiAl coating in 80wt.%V_2O_5– 20wt.%Na_2SO_4
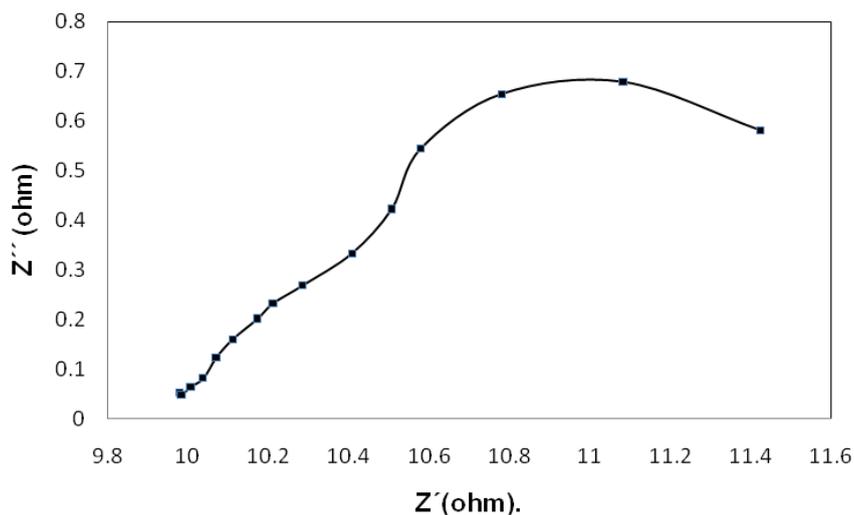

Figure 5. Nyquist Plots at 700°C, for the NiCrFeNbMoTiAl coating in 80wt.%V_2O_5– 20wt.%K_2SO_4

Previous research [4–21] have assessed the behaviour of the uncoated SAE213-T22 alloy when exposed to corrosive attack by molten salts, obtaining corrosion rate values higher than the obtained in

this research, allowing to infer that the coating applied during the development of this research did act as a thermal protective barrier.

C, Zeng, W. Wang, and W. Wu [22], defined an impedance model when protective layers formed on metallic surfaces that acted as thermal barriers decreasing the corrosive process; concluding that the process limiting factor was the ionic transport through the protective oxide layer rather than the diffusion of oxidizing species in the casting.
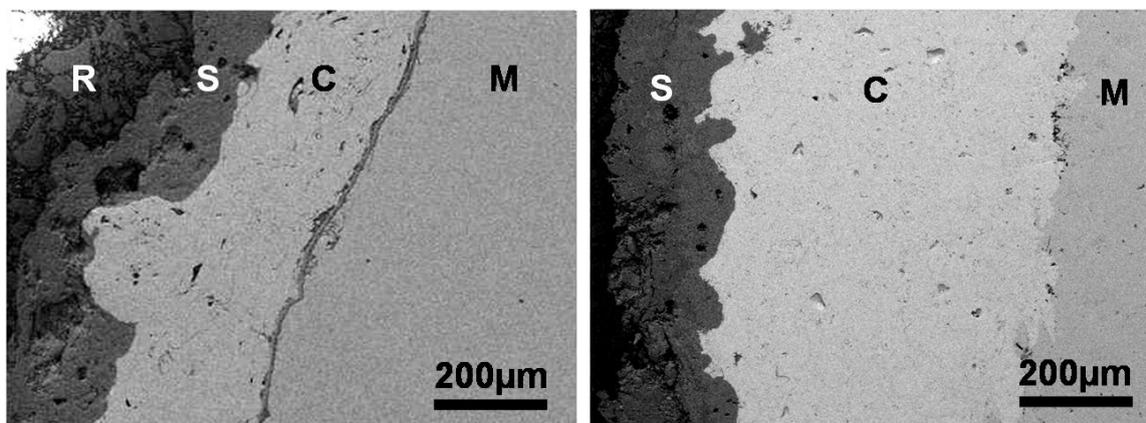

Figure 6. SEM micrograph 250X of coating after testing a) in $80\% V_2O_5 - 20\% Na_2SO_4$ and b) in $80\% V_2O_5 - 20\% K_2SO_4$, S=Salt, C=Coating, M=Matrix, R=Resin.

Table 5. Average thickness values of the coating.

Mixture	Initial Thickness (μm)	Final Thickness (μm)	Difference (μm)
$80\% V_2O_5 - 20\% Na_2SO_4$	210	156	54
$80\% V_2O_5 - 20\% K_2SO_4$	267	258	9

Scanning electron microscopy (SEM) corroborated that the higher intensity of attack presented when exposing the NiCrFeNbMoTiAl coating in the mixture composed by $80\% V_2O_5 - 20\% Na_2SO_4$, observing a larger deterioration and decrease in thickness of the coating layer than in the $80\% V_2O_5 - 20 K_2SO_4$ mixture. Figure 6 shows SEM micrographs after testing at 700°C.

The presence of components of the NiCrFeNbMoTiAl coating in the salt layer adhered to the sample after the test was determined by means of X-ray maps analysis, Figures 7 and 8, indicating that the coating layer was dissolved by direct action of the salts mixture in molten state; a greater deterioration of the coating layer in the $80\% V_2O_5 - 20\% Na_2SO_4$ was observed. On the other hand, the presence of the component elements of the saline mixtures in the metallic coating layer was not observed, allowing assuring that there is not any species diffusion from the saline deposit to the

coating, and therefore to the coating – metal base interface. In this manner, there is confirmation of the non presence of Warburg's impedance in the Nyquist plots.
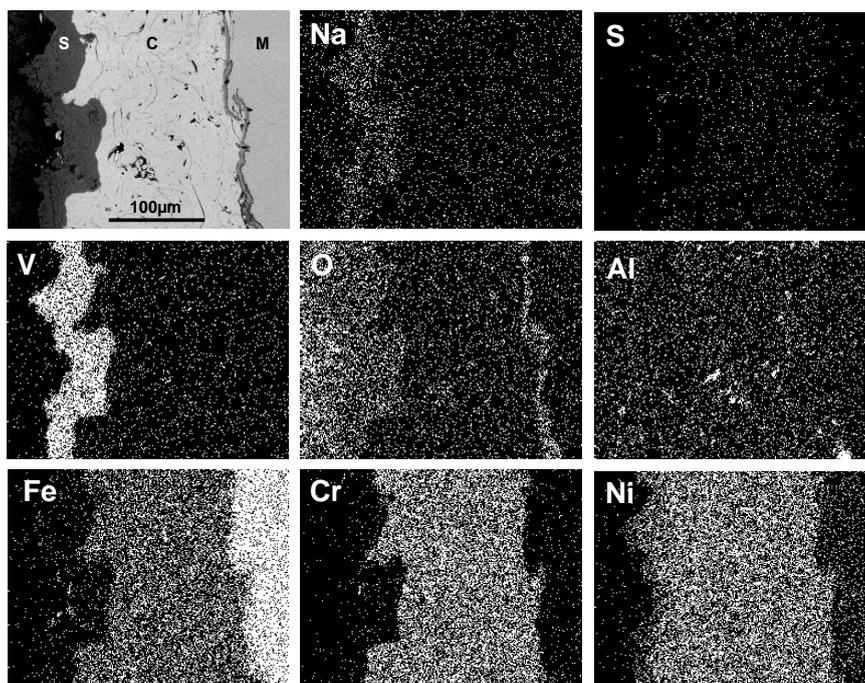
Figure 7. Cross-section backscattered image and X-ray maps of Na, S, V, O, Al, Fe, Cr and Ni after testing in $80\% V_2O_5 - 20\% Na_2SO_4$
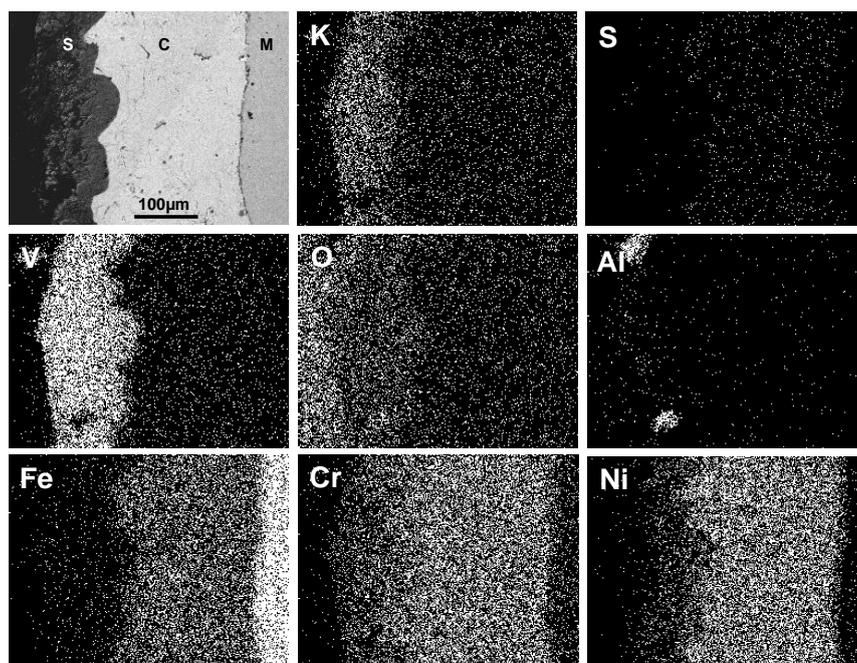
Figure 8. Cross-section backscattered image and X-ray maps of K, S, V, O, Al, Fe, Cr and Ni after testing in $80\% V_2O_5 - 20\% K_2SO_4$

Table 5 shows the average values of the coating layer thickness before and after each test; a greater decrease in thickness was observed when subjected to corrosive attack by molten salts in a $80\% V_2O_5 - 20\% Na_2SO_4$ mixture.
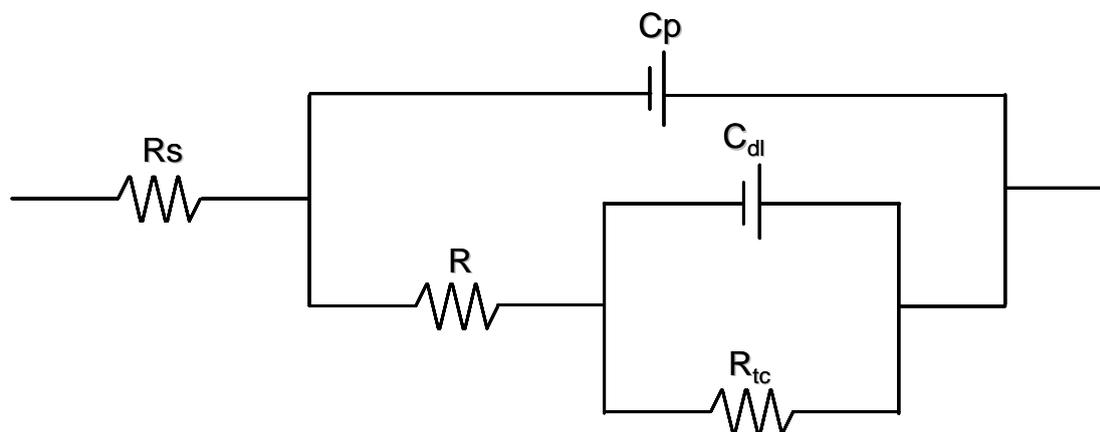

Figure 9. Equivalent electric circuit used to simulate the impedance results of the molten salts used.

Although the electric circuits are used as preliminary analysis for the corrosion mechanisms, it can be used to simulate the impedance data. According to the chemical stability of different metals in molten salts, they could present active or non-active behaviour. However, the common presented electrochemical mechanism on the surface is that the charge transfer controls the corrosion process, which could be described by an equivalent circuit with a double-layer capacitance Cdl at the coating/molten interface in parallel with the charge transfer resistance Rct which these were placed in series with the solution or electrolyte (the molten salt) resistance Rs. In a pure activation process, the double-layer capacitor corresponds to a perfect loop (as a perfect semicircle) in the EIS plot. On the other hand, if the coating is active and develops a scale, the charge transfer reaction can occur easily or slowly, depending upon the microstructure and chemical composition reactivity of corrosion products (figure 9).

4. CONCLUSIONS

The metallic coating NiCrFeNbMoTiAl, deposited by thermal projection assisted by non-transfer arc (APS) exposed to corrosive attack by molten salts composed of $80\% V_2O_5 - 20\% Na_2SO_4$ and $80\% V_2O_5 - 20\% K_2SO_4$ showed a good electrochemical behaviour.

The corrosive attack on the NiCrFeNbMoTiAl at 700°C became more severe when exposed to corrosion by molten salts in a mixture composed by $80\% V_2O_5 - 20\% Na_2SO_4$ decreasing the thickness of the sprayed layer in a larger proportion than when exposed to $80\% V_2O_5 - 20\% K_2SO_4$.

EDS analysis did not reveal the presence of elements of the mixture in the coating layer, confirming that it was the charge transfer mechanism the dominant factor in the activation process.

References

1. Cuevas. C, Porcayo. J, Izquierdo. G., *Corrosion Science* 46, (2004): p. 2663.
2. Soo-Haeng. C, Jin-Mok. H, Chung_Seok. S, Ji-Sup. Y, Seong-won. P*., Journal of Alloys and Compounds* 468, (2009): p. 263.
3. Almeraya-Calderon F, Matinez-Villafañe. A, González-Rodriguez JG., *British Corrosion Journal* 33, 4(1998): p 288.
4. Tristancho-Reyes J.L., "Evaluación de la corrosión en caliente de aleaciones, en un electrolito de $80\% V_2O_5 - 20\% Na_2SO_4$ entre 550 y 750°C por medio de métodos electroquímicos," Ms.C. diss., Escuela de Ingeniería Metalúrgica y Ciencia de los Materiales, Universidad Industrial de Santander – UIS., 2005.
5. N. Briks, G. Meier., "Introduction to high temperature oxidation of metals," (Cambridge, Cambridge University Press, 2006): p. 306.
6. Rapp. R, *Corrosion Science* 44, (2002): p. 209.
7. Rapp. R, Zhang. Y., JOM 46, 12(1994): p. 47.
8. Rapp. R, Goto. S., *Journal of the Electrochemical Society* 2, (1981): p. 159.
9. Goebel. J, Pettit. F, Goward. G., *Metallurgical Transactions* 4, (1973): p. 261.
10. Luthra. K, Spacil. H., *Journal of the Electrochemical Society* 2, (1982): p.64.
11. Sing. H, Prakash. S, Puri. D., *Surface and Coatings Technology* 192, (2005): p. 27.
12. Sidhu. B, Prakash. S., *Surface and Coatings Technology* 201, (2006): p. 1643.
13. R. Trevisan, C. Lima., "Aspersao térmica Fundamentaos e Aplicacioes," (Sao Pablo-Brasil, Artliber 2002): p. 85.
14. Matthews. S, James. B, Hyland. M., *Surface and Coatings Technology* 203, (2009): p. 1086.
15. ASTM G-102. Calculation of Corrosion Rates and Related Information from Electrochemical Measurements, American Society for Testing and Materials. USA. 1999.
16. ASTM G – 59. Standard Test Method for conducting Potentiodynamic Polarization Resistance measurements, American Society for Testing and Materials. USA. 1997.
17. ASTM G–3. Standard Practice for conventions applicable to Electrochemical Measurements in Corrosion Testing, American Society for Testing and Materials. USA. 1997.
18. Abdel Salam Hamdy, E. El-Shenawy and T. El-Bitar. *Int. J. Electrochem. Sci.,* 1(2006)171-180.
19. Mohammed A. Amin, Sayed S. Abd El-Rehim, E.E. F. El-Sherbini, and Rady S. Bayoumi. *Int. J. Electrochem. Sci*., 3 (2008) 199 - 215
20. Stern. M, Geary. A., *Journal of the Electrochemical Society* 104, (1957): p. 56.
21. Martinez–Villafañe. A, Almeraya-Calderon. F, Gaona-Tiburcio. C, Gonzales-Rodriguez JG, Porcayo-Calderon *J., JMEPEG* 7 (1998): p. 108.
22. Zeng. C, Wang. W, Wu. W., *Corrosion Science* 43, (2001): p. 787.